Energy Efficient Arrival with RTA Constraint for Multirotor eVTOL in Urban Air Mobility

Priyank Pradeep * and Peng Wei †
Iowa State University, Ames, IA, 50011

The electric vertical takeoff and landing (eVTOL) aircraft can alleviate transportation congestion on the ground by utilizing three-dimensional airspace efficiently. However, the endurance of Lithium-ion Polymer (Li-Po) batteries imposes critical constraints on the operational time span of an eVTOL aircraft on urban air mobility (UAM) passenger transportation mission. This research focuses on the formulation of fixed final time multiphase optimal control problem with energy consumption as the performance index for a multirotor eVTOL aircraft. The proposed multiphase optimal control problem formulation and the numerical solution enables a multirotor eVTOL aircraft to meet the assigned required time of arrival (RTA) and achieve an energy efficient arrival trajectory for a given concept of operation (CONOP), which is a critical enabler for the safe and efficient future eVTOL operations for passenger transportation and cargo delivery. The problem formulation is applied to a UAM passenger transportation use case with EHang 184 eVTOL aircraft, and an Uber proposed vertiport for five different types of CONOPs. Finally, the energy consumed for all the CONOPs is compared to propose the most energy efficient CONOP for a multirotor eVTOL on UAM passenger transportation mission. The proposed framework can also be used to address an energy efficient cargo delivery application in a UAS traffic management (UTM) context.

Nomenclature

A Rotor disk area

ATC Air traffic control

CTA Controlled time of arrival

D Drag force

$e(t)$ Instantaneous voltage across the motor

F_x Equivalent front plate area of the fuselage of the eVTOL aircraft

F_h Equivalent top plate area of the fuselage of the eVTOL aircraft

h Altitude of the aircraft

*Ph.D. Candidate, Aerospace Engineering Department, Howe Hall, 537 Bissell Rd and AIAA Student Member.
†Assistant Professor, Aerospace Engineering Department, Howe Hall, 537 Bissell Rd and AIAA Senior Member.

$i(t)$ Instantaneous current across the motor

J Optimal control performance index

m Mass of the aircraft

NAS National Airspace System

P Power

R Radius of the rotor

RTA Required time of arrival

T Thrust force

v_h Rotor induced velocity in hover

$(v_h)_e$ Co-axial rotor system effective induced velocity in hover

v_i Rotor induced velocity during forward flight

V True airspeed of the eVTOL aircraft

V_x Component of true airspeed along track

V_h Component of true airspeed along vertical direction

x Along track distance of the aircraft from the destination

α Angle of attack of air-stream relative to rotor tip path plane

γ Aerodynamic flight path angle

η Aerodynamic efficiency factor

θ Rotor tip-path-plane pitch angle

ρ Density of the air

ω_i Angular velocity of the i^{th} rotor

I. Introduction

Every day, millions of person-hours are spent unproductively in cities across the world due to road-traffic congestion. In 2014, the congestion caused 3.1 billion gallons of extra fuel burn in the US alone. Transportation as a whole accounted for approximately 33 % of CO_2 emissions in the US, of which 80 % were from cars and trucks traveling on the roadway system [1]. A study in the American Journal of Preventative Medicine, for example, found that those who commute more than 10 miles were at increased odds of elevated blood pressure [2]. The eVTOL aircraft can alleviate transportation congestion on the ground by utilizing three-dimensional airspace efficiently, just as skyscrapers allowed cities to use limited land more efficiently. The envisioned concept of urban air mobility (UAM) involves a network of small, electric aircraft that take off and land vertically (eVTOL), and, can enable rapid and reliable transportation

between suburbs and cities and, ultimately, within cities [3–5].

Recently, technological advances have made it possible to build and flight test eVTOL aircraft [3, 5, 6]. Over a dozen companies, for example, Airbus A^3, Aurora Flight Sciences, EHang, Jobby Aviation, Kitty Hawk, Leonardo, Lilium, Terrafugia, Volocopter, etc., with many different design approaches, are passionately working to make eVTOLs a reality. Despite various designs, they all have distributed electric propulsion (DEP) system in common. Considerable power-to-weight, efficiency, reliability and operational flexibility improvements are possible utilizing DEP technology in eVTOLs compared to the rotor system of conventional helicopters [3, 5–8]. The conventional helicopters are capable of VTOL, but the noise generated by them has been significant enough to compel communities to take legal action on their usage in UAM [6]. DEP powered eVTOLs have a higher downwash velocity compared to conventional helicopters that permits a more rapid vertical descent without entering a vortex ring state [3]. Engine failure accounts for 18 % of general aviation accidents when combined with fuel management errors. The use of DEP, controllers, and a redundant battery bus architecture avoids the problems of catastrophic engine failure by having full propulsion system redundancy [3, 5, 7]. The eVTOLs also have an advantage of zero operational emissions as they use electric propulsion [3, 5, 9].

In this paper, we present multiphase optimal control framework for a multirotor eVTOL aircraft (like CityAirbus, EHang 184 and Volocopter 2X) [10–12] to perform energy efficient arrival with required time of arrival (RTA) constraint for a given concept of operation (CONOP). The proposed multiphase optimal control problem formulation and the numerical solution are the critical enablers for the safe and efficient arrival of a multirotor eVTOL aircraft in on-demand UAM. Our problem formulation is applied to a UAM passenger transportation use case with EHang 184 eVTOL aircraft and an Uber proposed vertiport in numerical simulations. The proposed framework can also be used to address an energy efficient cargo delivery case in unmanned aircraft systems (UAS) traffic management (UTM) context.

II. Background and Motivation

A. Background

The commercial UAM operations have occurred in the United States since the 1940s in Los Angeles (LA) and New York City (NYC) using helicopters to transport people and mail between dozens of locations, but they ceased from LA and NYC in 1968 and 1977 respectively because of multiple tragic incidents [6]. However, current aviation technologies have reached a level of maturity to enable UAM using quiet and efficient manned and unmanned vehicles to conduct on-demand and scheduled operations [3, 5, 6]. At present, there is an increase in consumer demand in many cities worldwide towards developing an air taxi service in UAM environment [3, 6, 13]. Market research on UAM has shown that in the US alone, airport shuttle and air taxi markets have a market value of $ 500 billion at the market entry price points in the best-case unconstrained scenario [14].

Since 2013, NASA [9] and its collaborators from government, industry, and academia have contributed to the

research and development of UAS traffic management (UTM). They have been focused on small UAS operations, which include cargo delivery proposed by Amazon and Google. However, from 2016 onwards the possibility of urban air mobility (UAM) has also been explored by NASA and university researchers. Significant work has been performed towards defining high-level descriptions of both emergent and early expanded operational concepts for UAM [3, 5, 6, 9, 15]. Most of the UTM and UAM operations of eVTOLs are expected to be under limited battery endurance and vertiport capacity during early expanded UAM operations [6].

A few groups have worked on commercial jetliners for fuel-efficient and noise-abatement arrivals [16–24]; however, according to our knowledge, little research work has been carried out for the energy efficient arrival under time constrained environment for eVTOLs in UAM. This paper aims to fill this gap to enable safe and efficient multirotor eVTOL operations given limited vertiport capacity and eVTOL battery endurance.

B. Motivation

Studies and operational trials have been undertaken to investigate the performance and behavior of the assigned RTA for the fixed-wing aircraft [25–27]. The assigned RTA (control mechanism) enables aircraft to meet a controlled time of arrival (CTA) imposed by Air Traffic Control (ATC) at the meter fix [28]. The assigned RTA to the meter fix can be met either using speed adjustment strategy or path modification strategy or combination of both [24, 28, 29]. RTA improves air traffic operations by increasing the overall predictability of traffic that is easier to handle (fewer conflicts, information comes well in advance). Since the goals for integration of UAM with existing National Airspace System (NAS) includes imposing minimal additional: (i) workload on air traffic controllers and (ii) requirements or burdens on NAS [6]. Therefore, the precise implementation of 4D trajectory operations in UAM requiring each eVTOL aircraft to precisely follow 4D trajectory consisting of a planned 3D path (spatial) and an along-path time constraint will assure adequate separation between eVTOLs and optimize the use of limited NAS resources.

The energy required to complete a UAM mission by an eVTOL aircraft must be less than the energy available in Lithium-ion polymer (Li-Po) battery pack. Also, from the certification point of view eVTOL aircraft may require landing with reserve battery charge/usage time (analogous to reserve fuel in the aircraft). Though DEP is the preferred propulsion choice for the VTOL air taxi, the specific energy (the amount of energy per unit weight provided by the battery) of Li-Po batteries today is insufficient for long-range commutes [3, 6]. Therefore, planning and flying minimum energy trajectories is critical to safe and efficient UAM operations.

Hence, the research effort on UAM, need to address the following two critical operational challenges for passenger transportation and cargo delivery by the eVTOL aircraft:

(i) Generate the most energy efficient arrival trajectory given limited battery endurance.

(ii) Meet the assigned RTA constraint given the safe eVTOL aircraft separation and limited vertiport arrival time slots.

Therefore, the current research is motivated to generate an energy efficient arrival trajectory with RTA constraint for

a given CONOP and an eVTOL aircraft in UAM. Finally, the energy consumed for all the CONOPs is compared to propose the most energy efficient CONOP for a multirotor eVTOL on UAM passenger transportation mission.

III. Problem Formulation

A. eVTOL Aircraft Model

In this paper, the eVTOL aircraft is modeled based on specifications of EHang 184 [10]. However, the multiphase optimal control problem formulation presented in this paper can be easily modified and used for other multirotor eVTOL models such as CityAirbus [11] and Volocopter 2X [12].

EHang 184 has four arms with each arm consisting of two identical coaxial counter-rotating rotors (X8-configuration).

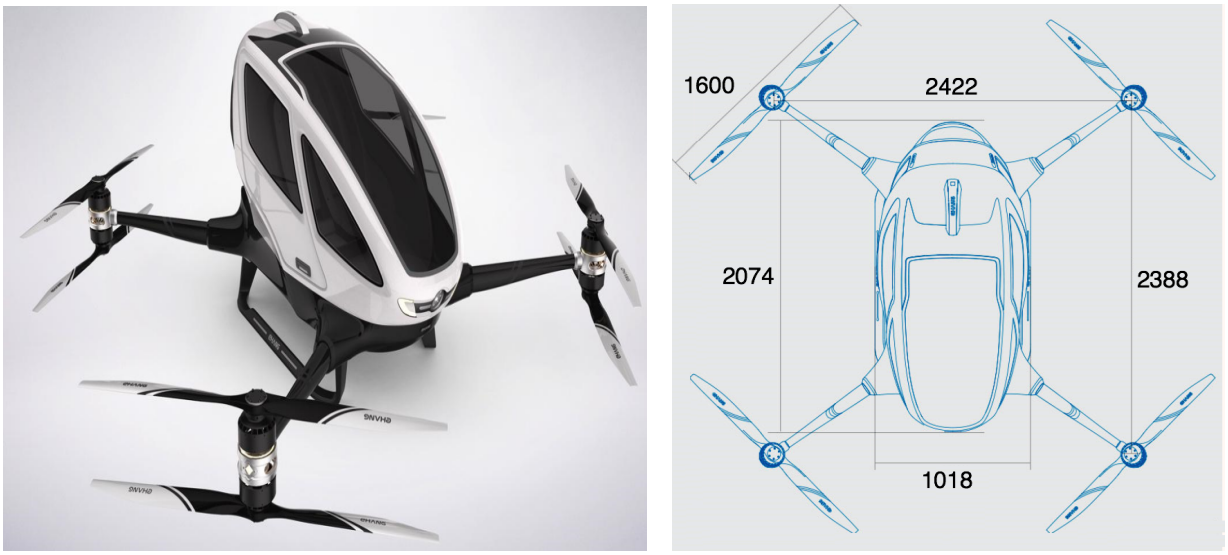

Fig. 1 EHang 184: coaxial multirotor eVTOL aircraft with X8-configuration [10]

B. Trajectory Optimization

The lateral path between the initial position of the eVTOL in-air (cruise phase) and the vertiport is assumed to be a geodesic path. Therefore, only the vertical trajectory of the eVTOL aircraft is free for optimization. However, since constraint has been imposed on the arrival time of eVTOL aircraft, the problem involves generation of an energy-optimal vertical path for the eVTOL aircraft with fixed final time. In this paper, the vertical trajectory optimization is formulated as a multiple phase optimal control problem of Lagrange type as follows [16, 30]:

$$J = \sum_{N=1}^{2} \int_{t_0^N}^{t_f^N} L^N(y(t), u(t), t)dt \tag{1}$$

subject to the first-order dynamic constraints:

$$\frac{dy(t)}{dt} = f^N(y(t), u(t), t) \tag{2}$$

subject to the path constraints:

$$C^N_{min} \leq C^N(y(t), u(t), t) \leq C^N_{max} \tag{3}$$

subject to the control bounds:

$$u^N_{min} \leq u(t) \leq u^N_{max} \tag{4}$$

where L is the Lagrangian cost function, N is the vertical flight phase (N = 1 for cruise and N = 2 for descent), y(t) is the state vector, u(t) is the control vector and C(y(t), u(t), t) represents the path constraints.

C. Flight Kinematics and Dynamics Model

In quadrotors roll, pitch and yaw angles are controlled by using various differential thrust mechanism across the rotors. For example, differential thrust between opposite motors provides roll and pitch moments [31]. Previously, researchers [32–34] have successfully decoupled longitudinal and lateral dynamics for helicopters with the conventional design. In general, quadrotors have a more symmetrical design (the location of rotors and the axis of rotation w.r.t center of gravity) than the conventional helicopters. Hence, to simplify the optimal control problem and reduce the computational time, the longitudinal dynamics of the multirotor eVTOL aircraft has been decoupled from lateral dynamics [32–34]. This allows us to solve the vertical trajectory generation problem as 2D flight dynamics problem in the vertical plane.

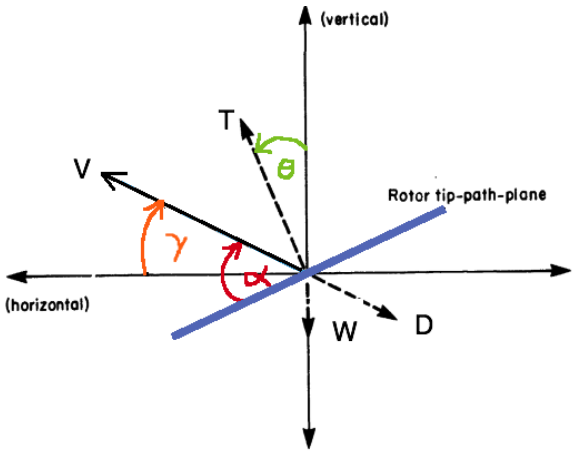

Fig. 2 Definition of the aircraft's position, velocity and forces

The two-dimensional longitudinal dynamics model of the aircraft in a fixed inertial frame of reference is as follows:

$$\frac{dV_x}{dt} = \frac{T\sin\theta - D\cos\gamma}{m} \tag{5}$$

$$\frac{dV_h}{dt} = \frac{T\cos\theta - D\sin\gamma - mg}{m} \tag{6}$$

$$\frac{dx}{dt} = V_x \tag{7}$$

$$\frac{dh}{dt} = V_h \tag{8}$$

$$T = \sum_{\mathrm{i}=1}^{4} (T_{\mathrm{arm}})_i \tag{9}$$

where [x,h] is the position vector (along track distance, altitude) of the center of mass relative to the origin (inertial frame of reference), θ is the rotor tip-path-plane pitch angle, T is the net thrust, D is the net drag, $(T_{\mathrm{arm}})_i$ is the net thrust produced by the i^{th} arm (two counter-rotating coaxial rotors), m is the mass, [V_x,V_h] are the horizontal and vertical components of the true airspeed and g is the acceleration due to gravity. Therefore, the state vector and control vector are defined as:

$$y(t) = [x, h, V_x, V_h]^T \tag{10}$$

$$u(t) = [\theta, T]^T \tag{11}$$

Also, the rotor tip-path-plane pitch angle (θ), the rotor angle of attack (α) and the eVTOL aircraft's flight path angle (γ) are related as following:

$$\alpha = \theta + \gamma \tag{12}$$

D. Drag Model

Based on the maximum ground speed of the aircraft (100 km/hr), the aircraft operates in M < 0.3 flow regime and hence the drag force on the fuselage of the eVTOL aircraft can be modeled based on the incompressible flow theory. The net drag on the aircraft is assumed to be equivalent to the drag on the fuselage of the aircraft. Therefore, the net drag on the aircraft is calculated as follows [33, 35]:

$$D = \frac{\rho V^2 C_D F}{2} \tag{13}$$

where F is the equivalent flat plate area of the fuselage and $C_D = 1$ [33].

The horizontal and vertical components of the drag in fixed inertial frame of reference are as follows:

$$D_x = \frac{\rho V_x^2 C_D F_x}{2} \tag{14}$$

$$D_h = \frac{\rho V_h^2 C_D F_h}{2} \tag{15}$$

where F_x and F_h are the equivalent front and top flat plate area of the fuselage respectively.

The performance data of EHang 184 used for aerodynamics and momentum theory related computations are as shown in Table 1:

Table 1 Performance Data

Variable	Value
Rotor Diameter (m)	1.6
Mass (kg)	240
Equivalent Front Plate Area (m^2)	2.11
Equivalent Top Plate Area (m^2)	1.47

E. Momentum Theory in Hover

Using momentum theory [31, 36, 37], the induced velocity (v_h) in hover is given by:

$$v_h = \sqrt{\frac{T_{\text{rotor}}}{2\rho A}} \tag{16}$$

where T_{rotor} is the thrust produced by the rotor, A is the rotor disk area (πR^2), R is the radius of the rotor and ρ is the density of the air.

F. Momentum Theory in Forward Flight

Consider a rotorcraft in forward motion at true airspeed V, with angle of attack α between the air-stream and the rotor disk (tip path plane). The solution for induced velocity (v_i) is [31, 36, 37]:

$$v_i = \frac{v_h^2}{\sqrt{(V\cos\alpha)^2 + (V\sin\alpha + v_i)^2}} \tag{17}$$

In forward flight, the thrust produced by an ideal isolated rotor per power input is given by [31, 36, 37]:

$$T_{\text{rotor}} = \frac{P_{\text{rotor}}}{V\sin\alpha + v_i} \tag{18}$$

The induced power loss of an isolated rotor ($P_{\text{induced rotor}}$) in forward flight is given by [31, 36, 37]:

$$P_{\text{induced rotor}} = T_{\text{rotor}} v_i \tag{19}$$

G. Coaxial Rotor Interference in Forward Flight

The eVTOL aircraft under consideration has 4 arms, with each arm consisting of two identical counter-rotating rotors. Assuming equal thrust produced by the lower and upper rotors of the coaxial rotor system, the net thrust produced by the arm (T_{arm}) is given by:

$$T_{\text{arm}} = T_{\text{lower}} + T_{\text{upper}} = 2T_{\text{rotor}} \tag{20}$$

Wing theory for a single lifting surface shows that the induced power loss of the arm i.e. coaxial counter-rotating system is [37]:

$$P_{\text{arm}} = 2P_{\text{induced rotor}}(1 + \chi) \tag{21}$$

where χ is the rotor interference factor for the coaxial rotor system. Typically, χ is ≤ 1. However, in the current research the interference factor (χ) for all the rotors is assumed to be 1.0 [37].

H. Power Required by the eVTOL aircraft

Energy balance equation for a multirotor eVTOL aircraft is given by [33, 38]:

$$\sum_{i=1}^{n} I_i \omega_i \frac{d\omega_i}{dt} = \sum_{i=1}^{n} P_i - P_{\text{required}} \tag{22}$$

where P_i is the energy supplied to the i^{th} rotor, P_{required} is the instantaneous power required by the aircraft (to overcome induced drag, profile drag, parasite drag and/or gravity to climb), ω_i is the rotational speed of the i^{th} rotor, I_i is the rotational moment of inertia of the i^{th} rotor and n is the total number of rotors on a multirotor eVTOL aircraft. However, based on assumption of quasi-steady flight in the current research, the instantaneous power required in forward flight is equal to the sum of the induced power, parasite power, climb power and profile power [36, 37, 39].

$$P_{\text{required}} = P_{\text{induced}} + P_{\text{parasite}} + P_{\text{climb}} + P_{\text{profile}} \tag{23}$$

The profile power exhibits only a slight increase in value with forward speed unless the tip of the rotor is above the critical Mach number [37]. Since the eVTOL aircraft considered in this research is a low speed aircraft with a small rotor diameter (1.6 m), the profile drag is assumed to be constant in magnitude and hence has a negligible impact on the variation of the instantaneous power required. Therefore, in the current research P_{required} is assumed to be [37]:

$$P_{\text{required}} = P_{\text{induced}} + P_{\text{parasite}} + P_{\text{climb}} \tag{24}$$

The induced power loss of the eVTOL aircraft (P_{induced}) is equal to the summation of the induced power loss of each arm (P_{arm}). Therefore, the induced power loss of the eVTOL aircraft is given by:

$$P_{\text{induced}} = \sum_{i=1}^{4} (P_{\text{arm}})_i \tag{25}$$

where $(P_{\text{arm}})_i$ is the induced power loss of the i^{th} arm as derived in equation 21.

The power required to climb and to propel the eVTOL aircraft forward (the parasite power loss) is given by [37]:

$$P_{\text{parasite}} + P_{\text{climb}} = TV \sin \alpha \tag{26}$$

where T is the net thrust, V is the true airspeed and α is the angle of attack of the tip-path-plane of the rotor.

Therefore, the instantaneous power required (P_{required}) in forward flight is given by:

$$P_{\text{required}} = \sum_{i=1}^{4} (P_{\text{arm}})_i + TV \sin \alpha \tag{27}$$

I. Performance Index of Multiphase Optimal Control

The power supplied by the battery pack to the ideal i^{th} motor at time t is given by [31]:

$$P_i(t) = e_i(t) i_i(t) \tag{28}$$

where $e_i(t)$ and $i_i(t)$ is the instantaneous voltage and current across the motor respectively [31, 40]. Therefore, by equating the total energy supplied by the battery pack to the ideal power consumed by all the motors (8 in total), the power consumed by the motors is given by:

$$P(t) = \sum_{i=1}^{8} e_i(t) i_i(t) \tag{29}$$

Hence from the above equation, we can see that in order to minimize battery usage the following performance index needs to be minimized (the Lagrange type problem):

$$J = \int_0^{t_f} \sum_{i=1}^{8} e_i(t) i_i(t) dt \tag{30}$$

The performance index of multiphase optimal control problem for the vertical trajectory optimization of the eVTOL aircraft is as follows:

$$J = \sum_{N=1}^{2} \int_{t_0^N}^{t_f^N} \sum_{i=1}^{8} e_i(t) i_i(t) dt \tag{31}$$

where N is the vertical flight phase (N = 1 for cruise and N = 2 for descent).

Assuming that the power supplied by the battery pack is equal to the power required (induced and parasite), ignoring the profile power, the performance index for the vertical trajectory optimization of the eVTOL aircraft is:

$$J = \sum_{N=1}^{2} \int_{t_0^N}^{t_f^N} (\sum_{i=1}^{4} (P_{\text{arm}})_i + TV \sin\alpha) dt \tag{32}$$

J. Path Constraints

The eVTOL aircraft's pitch angle is assumed to be bounded to 6° for passenger comfort based on discussions with experienced pilots.

$$-6^\circ \leq \theta_{\text{fuselage}} \leq 6^\circ \tag{33}$$

Therefore, in this research, collective pitch mechanism of a multirotor eVTOL, i.e., the collective changes to the pitch angle of the rotor-tip-path-plane of all the rotors are studied for the feasibility of a UAM mission without passenger discomfort.

The maximum speed (m/s), maximum cruise altitude (m) and total power (KW) is bounded based on specifications of EHang 184 [10]

$$0 \leq V_x \leq 27.78 \tag{34}$$

$$0 \leq h \leq 3500 \tag{35}$$

$$P_{\text{required}} \leq 152 \tag{36}$$

where P_{required} is defined in equation 27.

When a multirotor aircraft starts to descend from the cruise phase, the flow starts to develop recirculation near the disk and turbulence above it [37, 41]. However, at small rates of descent, the flow in the vicinity of the disk is still reasonably well represented by the momentum theory model. In vortex ring state, the flow near the rotor disk becomes highly unsteady and turbulent. Hence, the rotor in this state experiences a very high vibration level and loss of control. In order, to avoid the eVTOL aircraft entering into vortex ring state, the following path constraint has been imposed to the descent phase of the problem [37, 41]:

$$-0.28 \leq \frac{V \sin\alpha}{(v_h)_e} \leq 0 \tag{37}$$

$$(v_h)_e = \sqrt{\frac{2T_{\text{rotor}}}{2\rho A}} \tag{38}$$

where V is the true airspeed of the eVTOL aircraft, T_{rotor} is the thrust produced by the upper/lower rotor of the co-axial rotor system, $(v_h)_e$ is the effective induced velocity in hover of the co-axial rotor system and α is the angle of attack of

the tip-path-plane of the rotors.

The bounds on the two control variables of the multiphase optimal control problem: (i) rotor tip-path-plane pitch angle (θ) and (ii) Thrust (T) are discussed in section IV.

The cruise phase transitions to descent phase at Top of Descent (TOD) waypoint. Hence, TOD i.e. phase transition waypoint is subject to the phase link constraints on state variables (y) apart from the path and control constraints [30, 42] :

$$y^{N-1}(t_f^{N-1}) = y^N(t_0^N) \tag{39}$$

In our initial effort, airspace restrictions on the speed and altitude of the aircraft have been ignored. However, our framework allows us to easily modify bounds on the state and control variables based on new research findings about passenger comfortability and operational requirements.

K. Fixed Final Time

The implementation of RTA in the trajectory optimization (4D) of an eVTOL aircraft would be critical to the traffic management of UAM operations in future. In UAM operation, RTAs for individual eVTOL aircraft will be calculated by arrival scheduling algorithms [43, 44]. In the current research, RTA is imposed as final time constraint on the multiphase optimal control problem for eVTOL aircraft (EHang 184). Hence, the vertical trajectory optimization problem involves fixed final time (t_f) and position [x_f, h_f].

$$t_f = RTA \tag{40}$$

IV. Numerical Study

The equations of motion of the multirotor eVTOL aircraft (EHang 184) are continuous-time nonlinear differential equations which are difficult to solve analytically. For this reason, the vertical trajectory optimization problems are usually solved using direct collocation methods [16, 22]. A pseudospectral is a direct collocation method that transcribes a multiphase optimal control problem to a large sparse nonlinear programming (NLP) problem [30, 42]. We used GPOPS-II [30, 42] for transcribing the multirotor eVTOL's multiphase optimal control problem for a given CONOP to the corresponding NLP using hp-adaptive Gaussian quadrature collocation. The corresponding NLP is then solved using IPOPT [30, 42, 45].

As GPOPS and IPOPT may find a local optimum solution instead of the global optimum solution [46], therefore, five different types of CONOPs are numerically studied to understand and compare different airborne delay absorption strategies. The five CONOPs are as shown in Table 2 and Figure 3. Since the airborne delay is equal to the difference between the assigned RTA and nominal time of arrival [29] for a given aircraft type and CONOP, therefore, in this paper assigned RTAs are varied to study the impact of the airborne delay on energy consumption by EHang 184 for different

CONOPs.

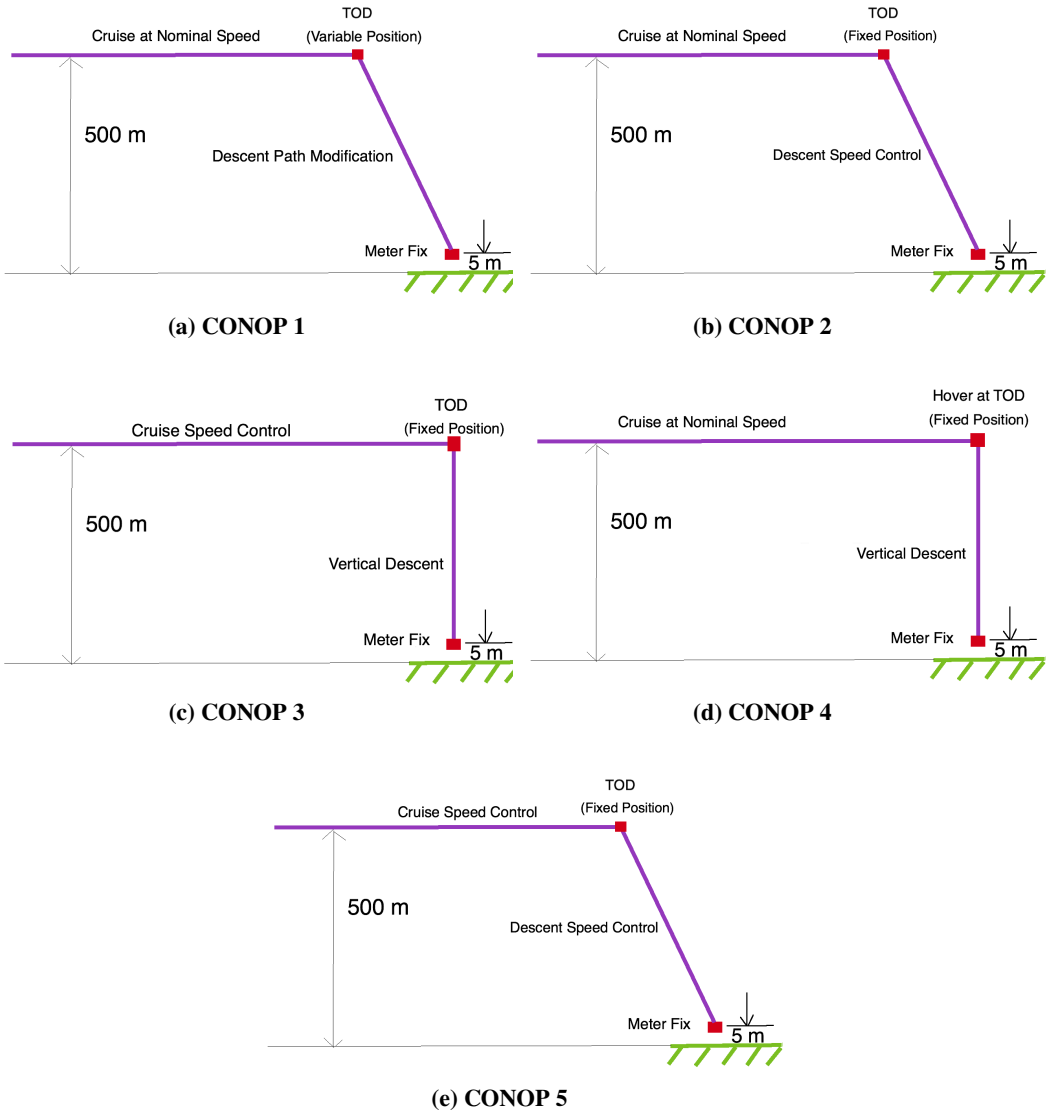

Fig. 3 CONOP 1 (delay absorption by descent path modification) vs. CONOP 2 (delay absorption by descent speed control) vs. CONOP 3 (delay absorption by cruise speed control) vs. CONOP 4 (delay absorption by hovering) vs. CONOP 5 (delay absorption using the combination of cruise and descent speed control)

As EHang 184 is a short range and slow speed eVTOL aircraft [3], the starting point for the fixed final time arrival trajectory optimization problem has been chosen as 20 km along-track distance from the vertiport. For all the CONOPs, the initial conditions (IC) and final conditions (FC) for the multiphase optimal control problem are as shown in Table 3. Since the initial altitude and final altitude of the eVTOL aircraft are greater than two times of rotor radius (2R), the in-ground effect (IGE) is neglected [37].

Table 2 Delay absorption strategies (CONOPs)

CONOP	Description
CONOP 1	Cruise at nominal speed followed by delay absorption primarily by descent path modification (variable TOD position).
CONOP 2	Cruise at nominal speed followed by delay absorption primarily by descent speed control (adjustment). The location of TOD is fixed.
CONOP 3	Delay absorption using cruise speed control (adjustment) followed by optimized vertical descent.
CONOP 4	Cruise at nominal speed followed by delay absorption using hover at TOD and then optimized vertical descent.
CONOP 5	Delay absorption using the combination of cruise speed control (adjustment) and descent speed control (adjustment) with equal distribution of delay to both the phases. The location of TOD is fixed.

Table 3 Initial and Final Conditions

State Variable	IC	FC
Altitude (m)	500	5
Along-track distance (m)	0	20000
Time (s)	0	RTA (t_f)

A. CONOP 1: Delay Absorption in Descent Phase (Variable TOD Position)

The first CONOP consists of cruise at nominal speed (27.78 m/s) [10] followed by descent as shown in Figure 3a. The location of TOD is computed by the numerical solver (GPOPS/IPOPT) of two-phase (cruise and descent) optimal control problem with fixed final time (i.e. assigned RTA). Hence, the airborne delay is mainly absorbed in descent phase by modification of the descent profile (vertical trajectory).

1. Energy Efficient Vertical Trajectories of the Fixed Pitch eVTOL aircraft

In this case study, the energy efficient trajectories are generated by assuming EHang 184 as a fixed pitch eVTOL aircraft. Further, the pitch angle of the fuselage of the eVTOL aircraft is assumed to be same as the pitch angle of the tip-path-plane of the rotors. Therefore, control bounds imposed on the pitch angle of the tip-path-plane of the rotors are based on passenger comfort ($-6^\circ \leq \theta_{\text{fuselage}} \leq 6^\circ$) as shown in Table 4.

Table 4 Lower and Upper Bounds on Control Variables

Control Variable	Lower Bound	Upper Bound
Rotor Pitch Angle (deg)	-6	6
Thrust (N)	0	4800

Figure 4, shows that for the energy efficient trajectories of CONOP 1, the airborne delays are progressively absorbed by shortening of the cruise segment followed by flying a shallower descent (i.e., TOD is computed further away from the destination) to meet the assigned RTAs. The sharp increase or decrease in control variables during the vertical phase transition in Figure 5, can be attributed to the problem formulation assumption of quasi-steady flight with point mass model for the eVTOL aircraft and numerical error due to using a less accurate numerical method, i.e., direct collocation method to solve the multiphase optimal control problem.

From Figure 4 and Figure 5, it can also be inferred that the lower and upper control bounds of +/- 6 degrees on the rotor pitch angle are insufficient to fly at 27.78 m/s, i.e., nominal cruise speed of EHang 184. As the results (computed cruise ground speeds) of the fixed pitch eVTOL aircraft is not in adherence to the proposed CONOP 1 for different RTAs, therefore, the results of this case study (fixed pitch mechanism) are not considered for energy consumption analysis. Thus, all onward case studies are carried out assuming that the eVTOL aircraft (EHang 184) has a collective pitch mechanism.

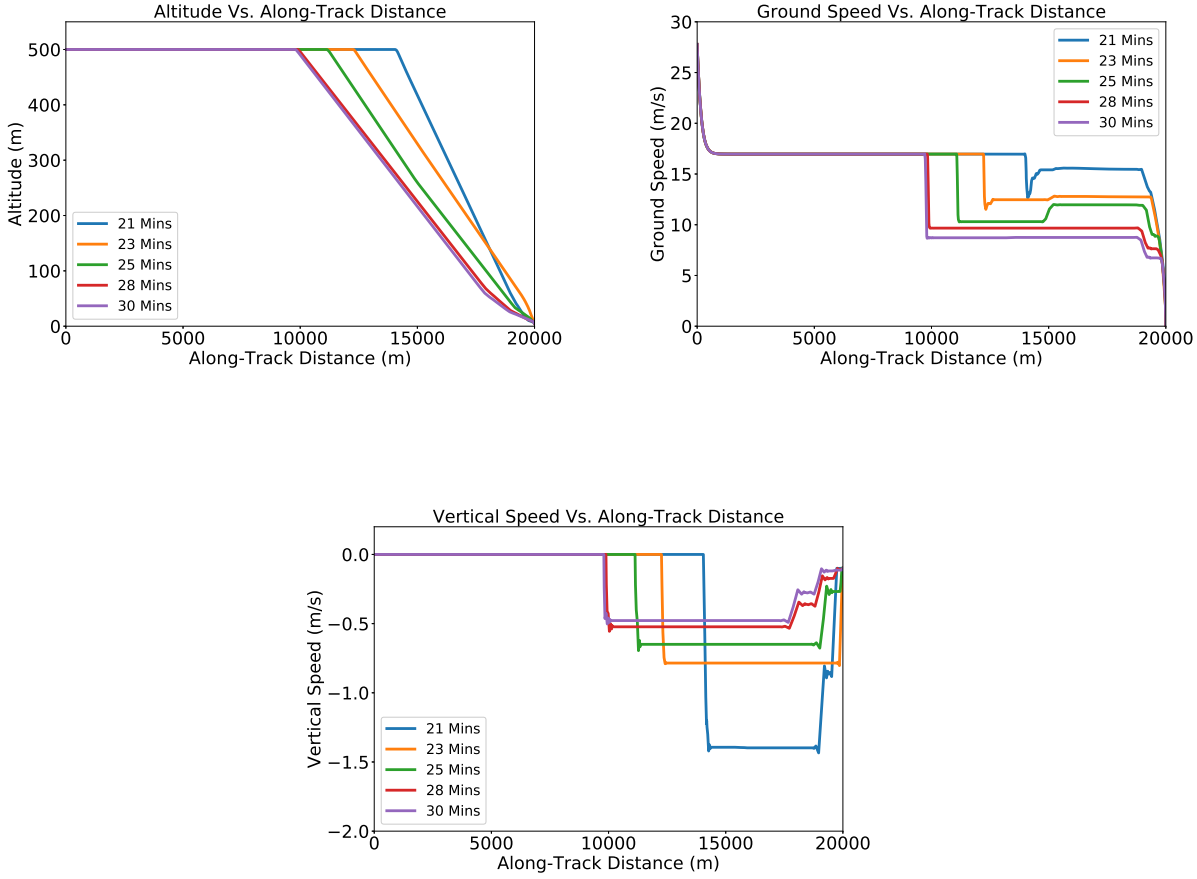

Fig. 4 CONOP 1: Energy efficient altitude, ground speed and vertical speed profiles of the fixed pitch eVTOL aircraft under various RTAs

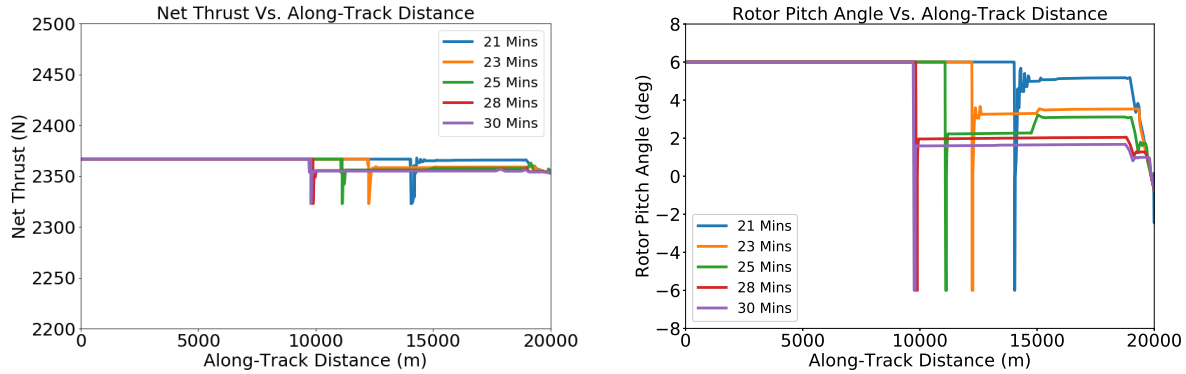

Fig. 5 CONOP 1: Energy efficient control strategy of the fixed pitch eVTOL aircraft under various RTAs

2. Energy Efficient Vertical Trajectories of the Collective Pitch eVTOL aircraft

As stated earlier, in this case study, the results are generated assuming the eVTOL aircraft has a collective pitch mechanism. Therefore, control bounds are not imposed on the pitch angle of the tip-path-plane of the rotors based on the passenger comfort as shown in Table 5.

Table 5 Lower and Upper Bounds on Control Variables

Control Variable	Lower Bound	Upper Bound
Rotor Pitch Angle (deg)	-25	25
Thrust (N)	0	4800

Unlike the previous case study, the ground speed for the cruise segment is computed as 27.78 m/s, i.e., EHang 184's nominal cruise speed. Therefore, Figure 6 and Figure 7 suggest that the collective pitch mechanism is required for the operational feasibility of a multirotor eVTOL aircraft like EHang 184 considering passenger comfort.

Figure 6, shows that for the energy efficient trajectories of CONOP 1; the airborne delays are progressively absorbed by shortening of the cruise segment followed by flying a shallower descent (i.e., TOD is computed further away from the destination) to meet the assigned RTAs. From Figure 8, it can be seen that with an increase in the airborne delays (assigned RTAs) the energy consumption is distributed more on to the descent phase than the cruise phase for CONOP 1. Therefore, the results of CONOP 1 show the advantage of using a shallower descent path (descent path modification strategy) for the airborne delay absorption.

As stated before, the sharp increase or decrease in control variables during the vertical phase transition can be attributed to the problem formulation assumption of quasi-steady flight with point mass model for the eVTOL aircraft and numerical error due to using a less accurate numerical method, i.e., direct method to solve the multiphase optimal control problem.

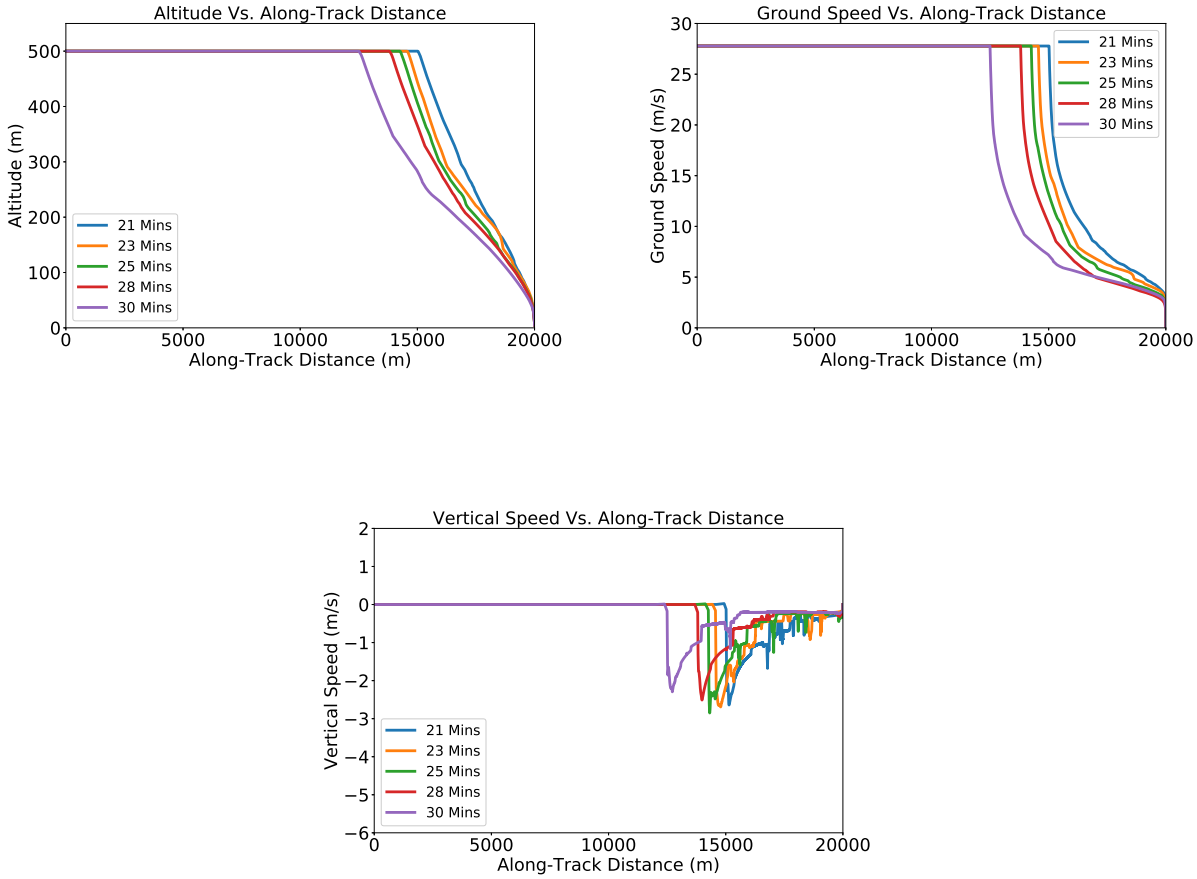

Fig. 6 CONOP 1: Energy efficient altitude, ground speed and vertical speed profiles of the collective pitch eVTOL aircraft under various RTAs

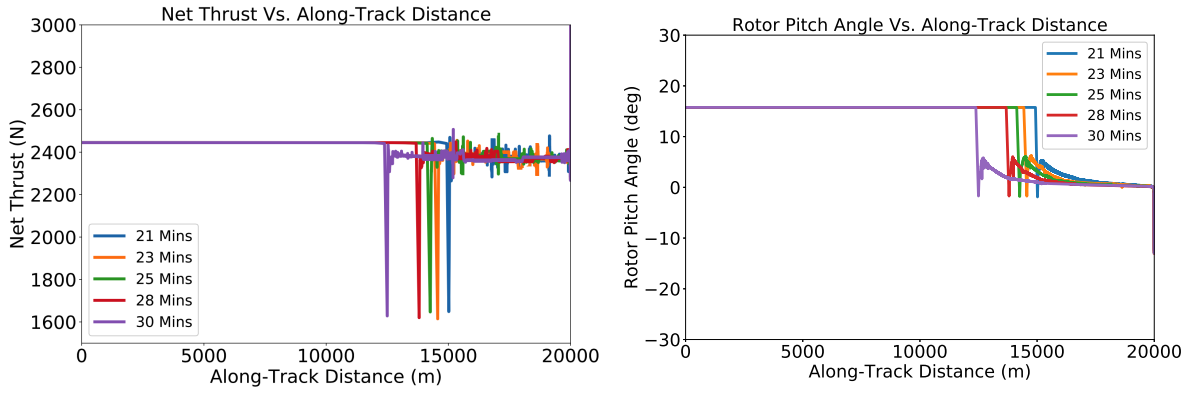

Fig. 7 CONOP 1: Energy efficient control strategy of the collective pitch eVTOL aircraft under various RTAs

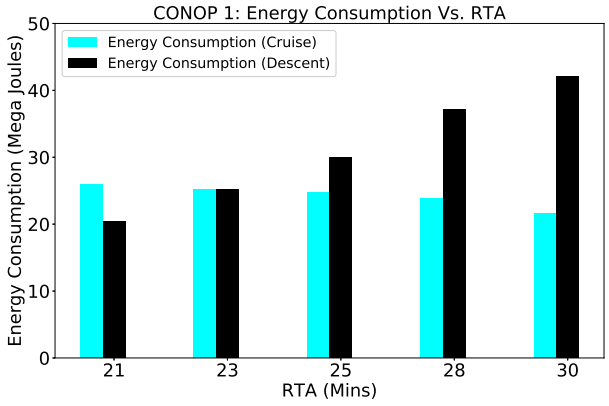

Fig. 8 CONOP 1: Energy consumption in cruise and descent phases under various RTAs

B. CONOP 2: Delay Absorption in Descent Phase (Fixed TOD Position)

The second CONOP consists of cruise at nominal speed (27.78 m/s) [10] followed by a shallow descent from fixed TOD position as shown in Figure 3b. The position of TOD is calculated at cruise altitude based on descent flight path angle of 3 degrees propagating in a backward direction from the meter fix (5 m above the vertiport). The numerical solver (GPOPS/IPOPT) is used to compute the descent profile (path and speed) to meet the assigned RTA. As stated earlier, in this case study, the energy efficient trajectories are generated by assuming EHang 184 has a collective pitch mechanism. From Figure 9, it can be seen that for CONOP 2, the airborne delay is efficiently absorbed primarily using descent speed control (adjustment) along with minor vertical path modification between the two fixed waypoints, i.e., TOD and the meter fix. Figure 10, indicates that with an increase in the airborne delays (assigned RTAs) the energy consumption in the descent phase increases whereas the energy consumption in the cruise phase remains the same as expected because of nominal cruise speed and fixed TOD position.

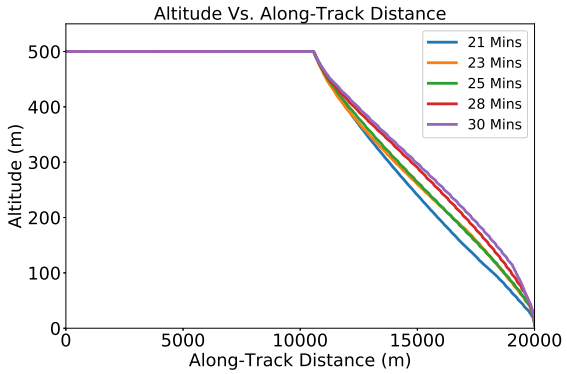

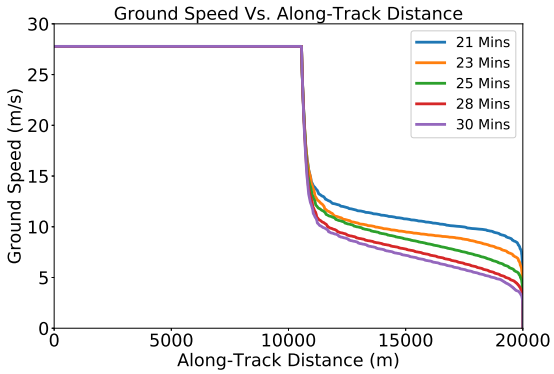

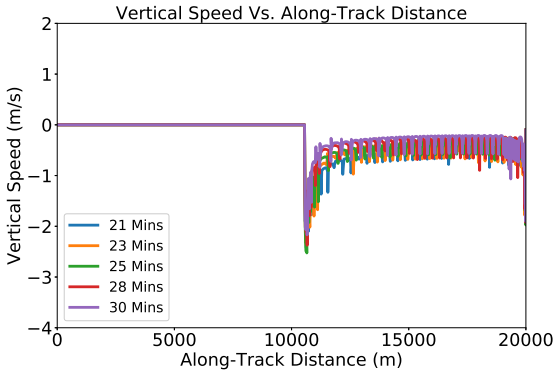

Fig. 9 CONOP 2: Energy efficient altitude, ground speed and vertical speed profiles of the collective pitch eVTOL aircraft under various RTAs

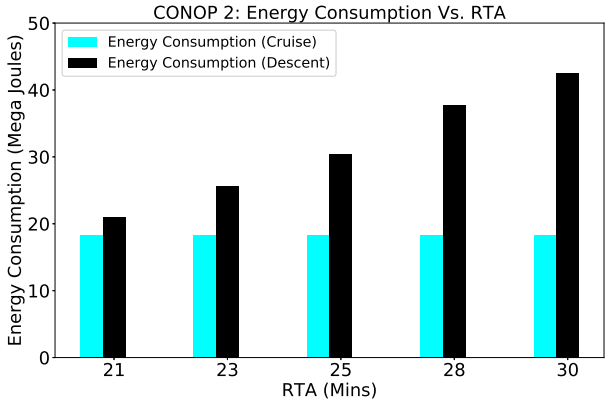

Fig. 10 CONOP 2: Energy consumption in cruise and descent phases under various RTAs

C. CONOP 3: Delay Absorption in Cruise Phase by Cruise Speed Control

The third CONOP consists of cruise at constant altitude followed by vertical descent as shown earlier in Figure 3c. In this case study, only cruise speed is adjusted to absorb the airborne delay. Hence, to compute cruise profile: (i) first, the flight duration (165.02 sec) for vertical descent from cruise altitude to the meter fix is computed using a single phase optimal control framework with energy as the performance index; and (ii) then the computed flight duration for vertical descent is imposed as time constraint on the descent phase of multiphase optimal control problem for all RTAs to generate trajectories. The following RTAs to the meter fix are imposed on the eVTOL: 21, 23, 25, 28 and 30 minutes. In this case study, the results are generated assuming the eVTOL aircraft has a collective pitch mechanism.

From Figure 11 and Figure 12, it can be seen that for CONOP 3, the airborne delays, i.e., increase in RTAs (21, 23, 25, 28 and 30 minutes) are energy efficiently absorbed by controlling the cruise speed without impacting the descent phase. Therefore, as shown in Figure 12, with an increase in the airborne delay (RTA) the energy consumption in the cruise phase increases while the energy consumption in the descent phase remains the same.

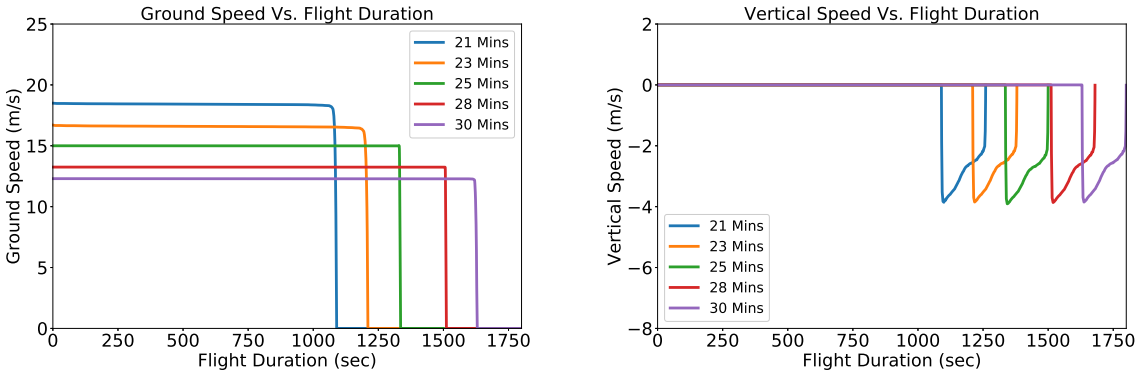

Fig. 11 CONOP 3: Time history of ground speed and vertical speed of the collective pitch eVTOL aircraft under various RTAs

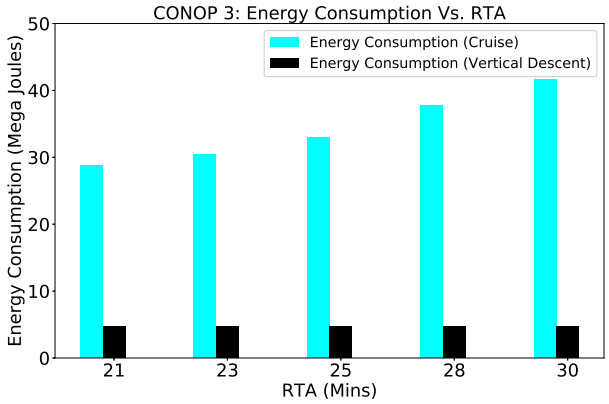

Fig. 12 CONOP 3: Energy consumption in cruise and vertical descent phases under various RTAs

D. CONOP 4: Delay Absorption in Hover at Cruise Altitude

The fourth CONOP consists of cruise at constant altitude and nominal speed (unlike cruise speed adjustment in CONOP 3) followed by the transition to hover at TOD to absorb the airborne delay and then vertical descent as shown earlier in Figure 3d. In this case study, only hover time is adjusted to absorb the airborne delay. Hence to compute hover time: (i) first, the flight duration (165.02 sec) for vertical descent from cruise altitude to the meter fix is computed using a single phase optimal control framework with energy as the performance index; (ii) next, the flight duration for the cruise phase is calculated assuming cruise at constant altitude and nominal cruise speed followed by the transition to hover at TOD; and (iii) finally, the computed flight durations for vertical descent and cruise are imposed as time constraints on the descent and cruise phases of multiphase optimal control problem to compute the hover time for a given RTA. The following RTAs to the meter fix are imposed on the eVTOL: 21, 23, 25, 28 and 30 minutes. In this case study, the results are generated assuming the eVTOL aircraft has a collective pitch mechanism.

From Figure 13, it can be seen that for CONOP 4, the airborne delay, i.e., increase in RTA (21, 23, 25, 28 and 30

minutes) is progressively absorbed in hover without impacting the cruise and descent phases. Therefore, as shown in Figure 13, with an increase in the airborne delay (RTA) the energy consumption in hover phase increases while the energy consumption in the cruise and descent phases remain the same.

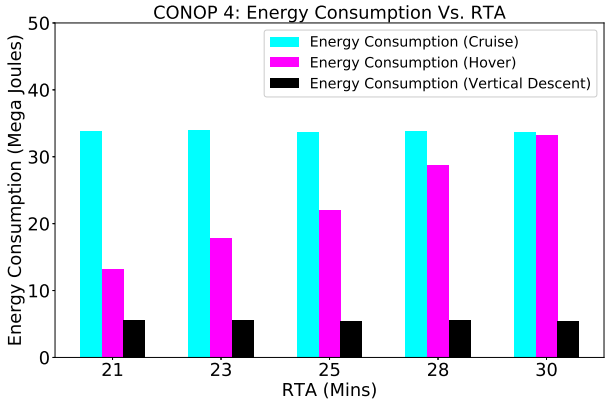

Fig. 13 CONOP 4: Energy consumption in cruise, hover and vertical descent phases under various RTAs

E. CONOP 5: Delay Absorption Using the Combination of Cruise and Descent Speed Control

The fifth CONOP consists of cruise at constant altitude followed by a shallow descent from fixed TOD position. The position of TOD is calculated at cruise altitude based on descent flight path angle of 3 degrees propagating in a backward direction from the meter fix (5 m above the vertiport). In this CONOP, the strategy is to equally distribute the airborne delay (assigned RTA) to both the phases. This strategy involves the combination of cruise speed control (adjustment) and descent speed control (adjustment) to absorb the airborne delay with minor vertical path modification between the two fixed waypoints (TOD and meter fix).

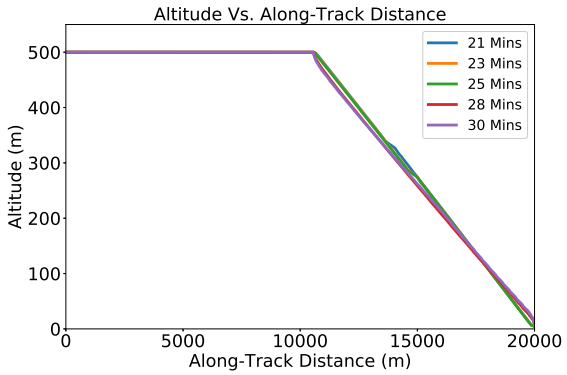

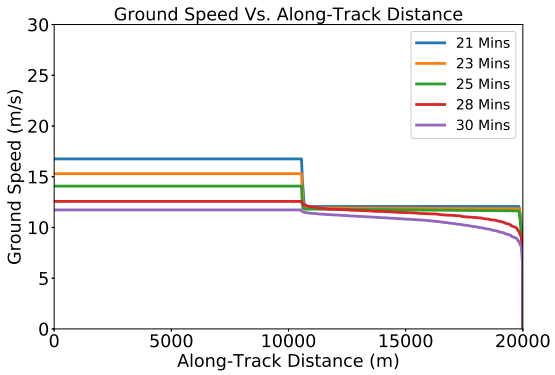

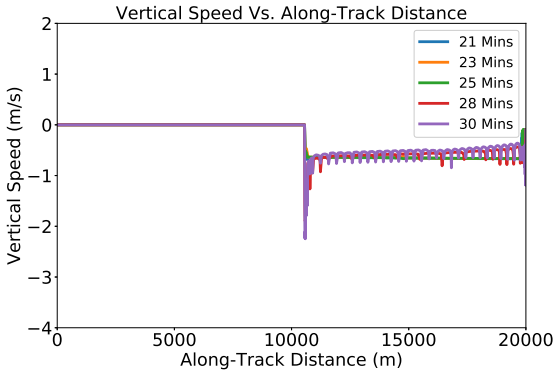

Fig. 14 CONOP 5: Energy efficient altitude, ground speed and vertical speed profiles of the collective pitch eVTOL aircraft under various RTAs

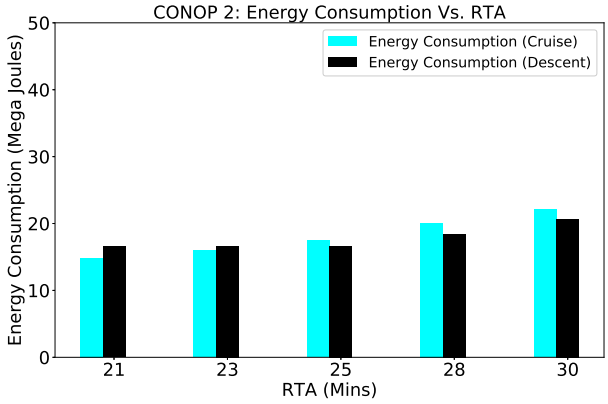

Fig. 15 CONOP 5: Energy consumption in cruise and descent phases under various RTAs

From Figure 14, it can be seen that for CONOP 5, the airborne delays, i.e., increase in RTAs (21, 23, 25, 28 and 30 minutes) are energy efficiently absorbed by controlling both the cruise speed and descent speed without much impact on the descent path. Therefore, as shown in Figure 15, with an increase in the airborne delay (assigned RTA) the energy consumption increases simultaneously in both the phases (cruise and descent).

F. Comparison of Total Energy Consumptions

From Figure 16, it can be observed that of the five CONOPs: (i) the least total energy consumption occurs in CONOP 5, i.e., the airborne delay absorption using the combination of cruise speed control and descent speed control with a shallow descent path to the meter fix; and (ii) the highest total energy consumption occurs in CONOP 4, i.e., the airborne delay absorption by hovering at TOD. Figure 16 also indicates that with an increase in flight duration there is an increase in the total energy consumption for all the CONOPs and therefore a clear need for higher stored energy in onboard Li-Po batteries of the eVTOL aircraft.

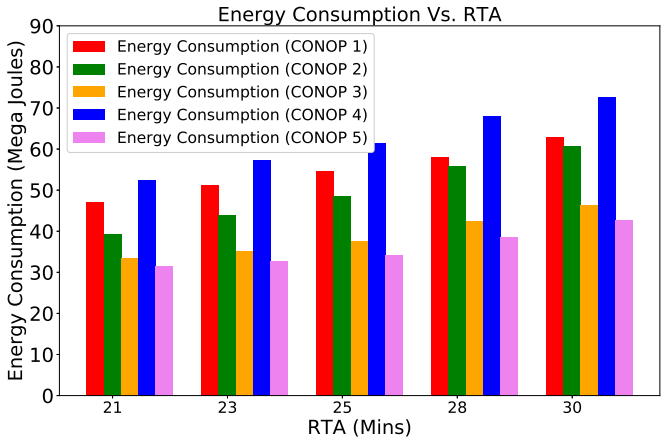

Fig. 16 Comparison of energy consumption for different CONOPs

V. Conclusions

In this research, multiphase optimal control problem with energy consumption as the performance index is formulated for a multirotor eVTOL aircraft (like CityAirbus, EHang 184 and Volocopter 2X) on an urban air mobility (UAM) passenger transportation mission. Further, we present a framework to perform energy efficient arrival for a multirotor eVTOL aircraft to meet the assigned required time of arrival (RTA) constraint in UAM for a given concept of operation (CONOP). The proposed framework can also be used to address an energy efficient cargo delivery case in a UAS traffic management (UTM) context.

The formulated vertical trajectory optimization problem is numerically solved using the pseudospectral method for a specific multirotor eVTOL aircraft, i.e., EHang 184 and five different types of CONOPs. The numerical results of the fixed pitch case study suggest that the collective pitch mechanism is required for the operational feasibility of a multirotor eVTOL aircraft like EHang 184 considering passenger comfort. Further, by imposing various arrival time constraints on the eVTOL aircraft, we found that for the energy efficient arrival operations, the airborne delay is best absorbed by CONOP 5, i.e., the combination of cruise speed control and descent speed control with a shallow descent path to the meter fix. The airborne delay absorption by hovering (CONOP 4) at the cruise altitude is the least energy efficient of all. Also, the numerical solutions showed that with an increase in flight duration there is an increase in the total energy consumption and therefore a clear need for higher stored energy in onboard Li-Po batteries of the eVTOL aircraft.

In the future, for a longer airborne delay absorption in early expanded and matured UAM operational environment, priority and weightage of the combination of the following three strategies: (i) cruise speed control, (ii) descent speed control and (iii) descent path modification, needs to be further investigated.

VI. Acknowledgment

The authors would like to especially thank Hokkwan Ng and Gilbert Wu at NASA Ames Research Center for their valuable advice. We are also thankful to Sang Gyun Park and Kshitij Mall for helping us in the usage of GPOPS-II/IPOPT.

References

[1] Schrank, D., Eisele, B., Lomax, T., and Bak, J., "2015 urban mobility scorecard," https://static.tti.tamu.edu/tti.tamu.edu/documents/mobility-scorecard-2015.pdf, 2015. [Online; accessed 18-January-2019].

[2] Hoehner, C. M., Barlow, C. E., Allen, P., and Schootman, M., "Commuting distance, cardiorespiratory fitness, and metabolic risk," *American journal of preventive medicine*, Vol. 42, No. 6, 2012, pp. 571–578. doi:10.1016/j.amepre.2012.02.020.

[3] Uber-Elevate, "Fast-forwarding to the future of on-demand, urban air transportation," https://www.uber.com/elevate.pdf, 2016. [Online; accessed 18-January-2019].

[4] Consulting, P., "The future of vertical mobility," https://fedotov.co/wp-content/uploads/2018/03/Future-of-Vertical-Mobility.pdf, 2018. [Online; accessed 18-January-2019].

[5] Airbus-A^3, "Vahana aero," https://vahana.aero/, 2018. [Online; accessed 14-November-2018].

[6] Thipphavong, D. P., Apaza, R., Barmore, B., Battiste, V., Burian, B., Dao, Q., Feary, M., Go, S., Goodrich, H. J., Kenneth H, Idris, H. R., Kopardekar, P. H., Lachter, J. B., Neogi, N. A., Ng, H. K., Oseguera-Lohr, R. M., Patterson, M. D., and Verma, S. A., "Urban air mobility airspace integration concepts and considerations," *2018 Aviation Technology, Integration, and Operations Conference*, 2018, p. 3676. doi:10.2514/6.2018-3676.

[7] Snyder, C. A., "Personal rotorcraft design and performance with electric hybridization," https://ntrs.nasa.gov/archive/nasa/casi.ntrs.nasa.gov/20170005655.pdf, 2017. [Online; accessed 18-January-2019].

[8] Kim, H. D., Perry, A. T., and Ansell, P. J., "A review of distributed electric propulsion concepts for air vehicle technology," *2018 AIAA/IEEE Electric Aircraft Technologies Symposium (EATS)*, IEEE, 2018, pp. 1–21. doi:10.2514/6.2018-4998.

[9] Prevot, T., Rios, J., Kopardekar, P., Robinson III, J. E., Johnson, M., and Jung, J., "UAS traffic management (UTM) concept of operations to safely enable low altitude flight operations," *16th AIAA Aviation Technology, Integration, and Operations Conference*, 2016, p. 3292. doi:10.2514/6.2016-3292.

[10] EHang-184, "EHANG 184 autonomous aerial vehicle specs," http://www.ehang.com/ehang184/specs/, 2018. [Online; accessed 14-November-2018].

[11] CityAirbus, https://www.airbus.com/newsroom/press-releases/en/2017/10/cityairbus-demonstrator-passes-major-propulsion-testing-mileston.html, 2017. [Online; accessed 18-January-2019].

[12] Volocopter, https://www.volocopter.com/en/urban-mobility/, 2018. [Online; accessed 18-January-2019].

[13] "Urban air mobility takes off in 64 towns and cities worldwide," https://www.unmannedairspace.info/urban-air-mobility/urban-air-mobility-takes-off-63-towns-cities-worldwide/, 2018. [Online; accessed 18-January-2019].

[14] "Urban air mobility (UAM) market study," https://www.nasa.gov/sites/default/files/atoms/files/bah_uam_executive_briefing_181005_tagged.pdf/, 2018. [Online; accessed 18-January-2019].

[15] Altawy, R., and Youssef, A. M., "Security, privacy, and safety aspects of civilian drones: A survey," *ACM Transactions on Cyber-Physical Systems*, Vol. 1, No. 2, 2016, p. 7. doi:10.1145/3001836.

[16] Park, S. G., and Clarke, J.-P., "Vertical trajectory optimization for continuous descent arrival procedure," *AIAA Guidance, Navigation, and Control Conference*, 2012, p. 4757. doi:10.2514/6.2012-4757.

[17] Robinson III, J., and Kamgarpour, M., "Benefits of continuous descent operations in high-density terminal airspace considering scheduling constraints," *10th AIAA aviation technology, integration, and operations (ATIO) conference*, 2010, p. 9115. doi:10.2514/6.2010-9115.

[18] Clarke, J.-P. B., Ho, N. T., Ren, L., Brown, J. A., Elmer, K. R., Tong, K.-O., and Wat, J. K., "Continuous descent approach: Design and flight test for Louisville International Airport," *Journal of Aircraft*, Vol. 41, No. 5, 2004, pp. 1054–1066. doi:10.2514/1.5572.

[19] Pradeep, P., and Wei, P., "Predictability, variability and operational feasibility aspect of CDA," *Aerospace Conference, 2017 IEEE*, IEEE, 2017, pp. 1–14. doi:10.1109/AERO.2017.7943728.

[20] Jin, L., Cao, Y., and Sun, D., "Investigation of potential fuel savings due to continuous-descent approach," *Journal of Aircraft*, Vol. 50, No. 3, 2013, pp. 807–816. doi:10.2514/1.C032000.

[21] Cao, Y., DeLaurentis, D., and Sun, D., "Benefit and trade-off analysis of continuous descent approach in normal traffic conditions," *Transportation Research Record: Journal of the Transportation Research Board*, , No. 2325, 2013, pp. 22–33. doi:10.3141/2325-03.

[22] Dalmau, R., Verhoeven, R., de Gelder, N., and Prats, X., "Performance comparison between TEMO and a typical FMS in presence of CTA and wind uncertainties," *2016 IEEE/AIAA 35th Digital Avionics Systems Conference (DASC)*, 2016, pp. 1–8. doi:10.1109/DASC.2016.7778097.

[23] Coppenbarger, R. A., Mead, R. W., and Sweet, D. N., "Field evaluation of the tailored arrivals concept for datalink-enabled continuous descent approach," *Journal of Aircraft*, Vol. 46, No. 4, 2009, p. 1200. doi:10.2514/1.39795.

[24] Xu, Y., and Prats, X., "Including linear holding in air traffic flow management for flexible delay handling," *Journal of Air Transportation*, 2017, pp. 123–137. doi:10.2514/1.D0081.

[25] Wing, D., "A potentially useful role for airborne separation in 4D-trajectory ATM operations," *AIAA 5th ATIO and16th Lighter-Than-Air Sys Tech. and Balloon Systems Conferences*, 2005, p. 7336. doi:10.2514/6.2005-7336.

[26] Prevot, T., Lee, P., Callantine, T., Smith, N., and Palmer, E., "Trajectory-oriented time-based arrival operations: Results and recommendations," *ATM2003, FAA/Eurocontrol R&D Seminar, Budapest, Hungary*, Citeseer, 2003.

[27] Coppenbarger, R., Lanier, R., Sweet, D., and Dorsky, S., "Design and development of the en route descent advisor (EDA) for conflict-free arrival metering," *AIAA Guidance, Navigation, and Control Conference and Exhibit*, 2004, p. 4875. doi: 10.2514/6.2004-4875.

[28] Smedt, D. d., Bronsvoort, J., and McDonald, G., "Controlled time of arrival feasibility analysis," `http://icrat.org/seminarContent/seminar10/papers/242-De%20Smedt_0126131150-Final-Paper-4-17-13.pdf`, 2013. [Online; accessed 18-January-2019].

[29] Nikoleris, T., Chatterji, G. B., and Coppenbarger, R. A., "Comparison of fuel consumption of descent trajectories under arrival metering," *Journal of Aircraft*, Vol. 53, No. 6, 2016, pp. 1853–1864. doi:10.2514/1.C033374.

[30] Rao, A. V., Benson, D. A., Darby, C., Patterson, M. A., Francolin, C., Sanders, I., and Huntington, G. T., "Algorithm 902: GPOPS, a matlab software for solving multiple-phase optimal control problems using the gauss pseudospectral method," *ACM Transactions on Mathematical Software (TOMS)*, Vol. 37, No. 2, 2010, p. 22. doi:10.1145/1731022.1731032.

[31] Hoffmann, G., Huang, H., Waslander, S., and Tomlin, C., "Quadrotor helicopter flight dynamics and control: Theory and experiment," *AIAA Guidance, Navigation and Control Conference and Exhibit*, 2007, p. 6461. doi:10.2514/6.2007-6461.

[32] Bottasso, C. L., Croce, A., Leonello, D., and Riviello, L., "Rotorcraft trajectory optimization with realizability considerations," *Journal of Aerospace Engineering*, Vol. 18, No. 3, 2005, pp. 146–155. doi:10.1061/(ASCE)0893-1321(2005)18:3(146).

[33] Yomchinda, T., Horn, J., and Langelaan, J., "Flight path planning for descent-phase helicopter autorotation," *AIAA Guidance, Navigation, and Control Conference*, 2011, p. 6601. doi:10.2514/6.2011-6601.

[34] Johnson, W., "Helicopter optimal descent and landing after power loss," 1977.

[35] DeMoss, J. A., "Drag measurements on an ellipsoidal body," Ph.D. thesis, Virginia Tech, 2007.

[36] Heyson, H. H., "A momentum analysis of helicopters and autogyros in inclined descent, with comments on operational restrictions," 1975.

[37] Johnson, W., *Helicopter theory*, Courier Corporation, 2012.

[38] Pradeep, P., Park, S. G., and Wei, P., "Trajectory optimization of multirotor agricultural UAVs," *2018 IEEE Aerospace Conference*, 2018, pp. 1–7. doi:10.1109/AERO.2018.8396617.

[39] Leishman, J., *Principles of helicopter aerodynamics*, Cambridge Aerospace Series, Cambridge University Press, 2002. URL `https://books.google.com/books?id=-PnV2JuLZi4C`.

[40] Morbidi, F., Cano, R., and Lara, D., "Minimum-energy path generation for a quadrotor UAV," *Robotics and Automation (ICRA), 2016 IEEE International Conference on*, IEEE, 2016, pp. 1492–1498. doi:10.1109/ICRA.2016.7487285.

[41] Chenglong, L., Zhou, F., Jiafang, W., and Xiang, Z., "A vortex-ring-state-avoiding descending control strategy for multi-rotor UAVs," *Chinese Control Conference (CCC), 2015 34th*, IEEE, 2015, pp. 4465–4471. doi:10.1109/ChiCC.2015.7260330.

[42] Garg, D., Patterson, M., Hager, W. W., Rao, A. V., Benson, D. A., and Huntington, G. T., "A unified framework for the numerical solution of optimal control problems using pseudospectral methods," *Automatica*, Vol. 46, No. 11, 2010, pp. 1843–1851. doi:10.1016/j.automatica.2010.06.048.

[43] Kleinbekman, I., Mitici, M. A., and Wei, P., "eVTOL arrival sequencing and scheduling for on-demand urban air mobility," *Digital Avionics Systems Conference, 2018 IEEE/AIAA*, IEEE/AIAA, 2018. doi:10.1109/DASC.2018.8569645.

[44] Pradeep, P., and Wei, P., "Heuristic approach for arrival sequencing and scheduling for eVTOL aircraft in on-demand urban air mobility," *Digital Avionics Systems Conference, 2018 IEEE/AIAA*, IEEE/AIAA, 2018. doi:10.1109/DASC.2018.8569225.

[45] Wächter, A., and Biegler, L. T., "On the implementation of an interior-point filter line-search algorithm for large-scale nonlinear programming," *Mathematical programming*, Vol. 106, No. 1, 2006, pp. 25–57. doi:10.1007/s10107-004-0559-y.

[46] Gauntt, R. D., "Aircraft course optimization tool using GPOPS matlab code," Tech. rep., Air Force Institute of Technology, 2012.